Indian Journal of Chemistry
Vol. 64, October 2025, pp. 933-941
DOI: 10.56042/ijc.v64i10.22854

Synthesis and evaluation of isatin-N-1,2,3-triazoles analogues for *in vitro* anticancer, α-glucosidase inhibition properties *via* molecular hybridization approach

A Niranjana Kumar[a], J Kotesh Kumar*[a], K V N S Srinivas*[a], Srinivas Chinde[b], Anand Kumar Domatti[c], Yogesh Kumar[d], Paramjit Grover[b], Ashok Tiwari[c] & Feroz Khan[d]

[a] Phytochemistry Division, CSIR-Central Institute of Medicinal and Aromatic Plants, Research Centre, Boduppal, Hyderabad 500 092, India

[b] Toxicology Unit, Biology Division, CSIR-Indian Institute of Chemical Technology, Hyderabad 500 007, India

[c] Medicinal Chemistry and Pharmacology Division, CSIR-Indian Institute of Chemical Technology, Hyderabad 500 007, India

[d] Metabolic and Structural Biology Department, CSIR-Central Institute of Medicinal and Aromatic Plants, Lucknow 226 015, India

E-mail: koteshkumarj.cimap@csir.res.in, kvnsatyasrinivas.cimap@csir.res.in

Received 18 August 2025; accepted (revised) 7 October 2025

The anticancer, α-glucosidase inhibition profiles of isatin-1,2,3-triazole conjugates (9 Nos) are reported here. The compounds **3a** (IC_{50} 6.52±0.04)**, 3b** (IC_{50} 2.78±0.04 μM), **3d** (IC_{50} 7.09±0.037 μM) and **3h** (2.25±0.04 μM) have shown more potent anti-cancer activity against HeLa and HepG2 cell lines respectively compared to the standard Doxorubicin (IC_{50} 9.03±0.07 and 10.15±0.003 respectively). While, compound **3e** potentially inhibits α-glucosidase enzyme (47.4%) when compared to the standard Acarbose (56.0%), compound **3f** has shown potent lipase inhibition activity (80.8%) when compared to the standard Orlistat (91.1%). In *in silico* studies, the docking of derivatives with the respecting anticancer, AGH and lipase targets have revealed their potential binding affinities. Also the plot of PSA *vs* ALogP has revealed the compounds with favorable physicochemical properties for CNS drug development or oral delivery.

Keywords: Isatin, 1,2,3-Triazole, Anticancer, α-Glucosidase, Lipase, Docking studies

Isatin (1*H*-indole-2,3-dione moiety) is one of the most promising class of heterocyclic molecule and consists of indole nucleus and two types of carbonyl groups *i.e*. keto and lactam groups. It can be found in plants of the genus *Isatis*[1], *Calanthe discolor* LINDL[2], and *Couroupita guianensis* Aubl[3]. Isatin also present in mammalian tissues, fluids[4] parotid gland of *Bufo* frogs.

Isatin is an extensible substrate that may be utilized to synthesize a wide range of heterocyclic compounds, such as amides and sulphonamides (carbonic anhydrase)[5], spiro compounds (antiproliferative)[6], urea/thiourea-based-derivatives (multi-kinase inhibitor)[7], schiff bases and oximes (*in vivo* antitumour activity)[8], metal ligands (antiproliferative)[9], indirubin analogues (antiproliferative)[10], di- or trisubstituted isatins (antiproliferative)[11], dihydropyrazole hybrids (antiproliferative)[12], Ciprofloxacin and Moxifloxacin hybrids (antimycobacterial)[13], ferrocene-tethered hybrids (antimycobacterial)[14], *etc*. Several isatin-based analogues have entered clinical studies, including two molecules, Sunitinib and Toceranib, that have been authorized for clinical usage against tumors. Other derivatives, including Nintedanib, Semaxinib, and Orantinib, are now in clinical studies for their anticancer potential (Fig. 1).

Assuming that the majority of isatin derivatives have antiproliferative abilities, the current study attempts to investigate the anti-cancer profile of isatin-1,2,3-triazoles (**3a-i**; 9 Nos) in addition to their α-glucosidase and lipase inhibition abilities.

Results and Discussion

Chemistry

The synthetic strategy of isatin N-substituted 1,2,3-triazoles was outlined in our earlier studies[15].

In vitro anti-cancer activity

Anticancer activity of Isatin-N-1,2,3-triazole derivatives **3a-i** were evaluated in *in vitro* mode[16] on the human cancer cell lines A549, HepG2, MCF-7, HeLa and SKOV3. The results of *in vitro* cytotoxic activity were expressed as the IC_{50} (μM) and doxorubicin was used as positive control (Table 1).

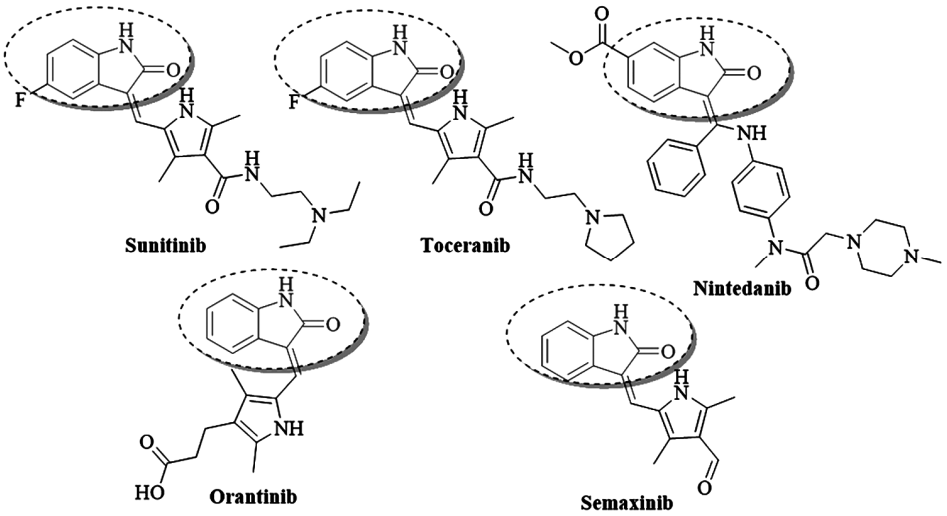

Fig. 1 — Structures of isatin derivatives approved as drugs or in clinical trials

Table 1 — Anticancer, α-Glucosidase and lipase inhibition activity of Isatin 1,2,3 triazole derivatives

Compd	*In vitro* anticancer activity (IC_{50} in μM)					Percentage of AGH Inhibition at 20 μg/mL	Percentage of Lipase Inhibition at 50 μg/mL
	A549	HepG2	MCF-7	HeLa	SKOV3		
3a	> 100	26.27±0.05	> 100	6.52±0.04	> 100	7.2	NA
3b	> 100	> 100	> 100	2.78±0.04	> 100	ND	44.4
3c	> 100	> 100	> 100	28.85±0.29	49.65±0.02	18.5	48.1
3d	7.72±0.07	7.09±0.037	> 100	> 100	> 100	35.6	26.4
3e	> 100	> 100	> 100	> 100	> 100	47.4	NA
3f	> 100	> 100	> 100	> 100	> 100	18.2	80.8
3g	> 100	> 100	> 100	> 100	> 100	15.8	30.7
3h	> 100	2.25±0.04	> 100	88.16±0.01	> 100	31.3	61.8
3i	> 100	> 100	> 100	> 100	> 100	25.0	NA
Doxorubicin	0.14±0.002	10.15±0.003	5.73±0.06	9.03 ±0.07	16.37±0.02	–	–
Acarbose	–	–	–	–	–	56.0	–
Orlistat	–	–	–	–	–	–	91.1

The compounds **3a** (IC_{50} 6.52±0.04 μM)**, 3b** (IC_{50} 2.78±0.04 μM) in which triazole ring attached to phenyl group were more potent specifically against HeLa cancer cell line, whereas compounds **3d** (IC_{50} 7.09±0.037 μM) and **3h** (IC_{50} 2.25±0.04 μM) with benzyl-triazole ring linkage shown more potent activity specifically against HepG2 cell line compared to the standard Doxorubicin (IC_{50} 9.03 ±0.07μM and 10.15±0.003 μM respectively) (Fig. 2). All the compounds (except **3d** and **3c)** in which triazole ring linked either to phenyl or benzyl ring shown no activity against MCF-7, A549 and SKOV3 cell lines. Compound **3c** with *para* nitro substituted bezyl-triazole ring shown moderate activity against HeLa and SKOV3 cell lines respectively (IC_{50} 28.85±0.29 and 49.65±0.02 μM) and **3d** with *meta* chloro-benzyl ring shown moderate activity against A549 and HepG2 cell lines.

Erythrocyte Osmotic Fragility

The erythrocyte osmotic fragility curve in Fig. 3 compares the haemolytic behaviour of anti-cancer active derivatives 3a, 3b, 3d, and 3h with quercetin, dimethyl sulfoxide (DMSO), and a control. The x-axis represents the percentage of phosphate-buffered saline (PBS), indicating decreasing osmolarity, while the y-axis shows the percentage of haemolysis. The control (black line) exhibits the least haemolysis, suggesting intact erythrocyte membrane stability. DMSO (orange line) follows a similar trend, indicating minimal membrane disruption. The isatin-1,2,3-triazole derivatives display varying degrees of fragility; compounds 3a (blue), 3b (red), 3d (purple), and 3h (light blue) show increased haemolysis at lower saline concentrations, with 3d exhibiting the highest fragility among them. The differences in fragility curves indicate that isatin-1,2,3-triazole derivatives interact

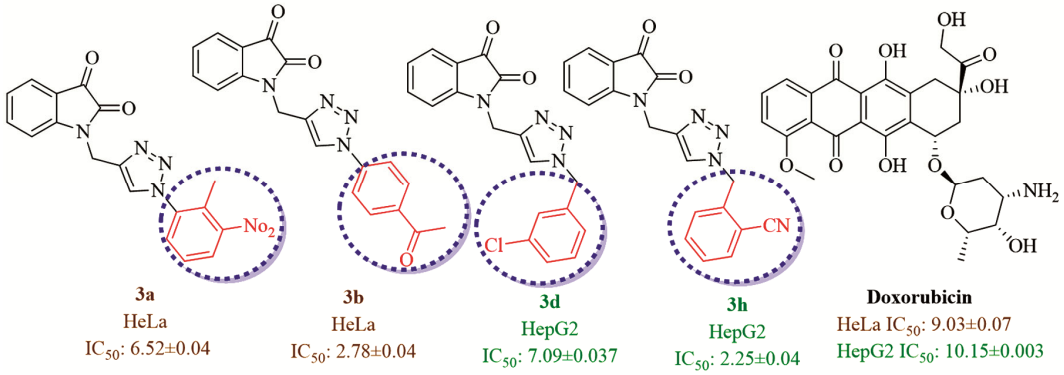

Fig. 2 — Structures of more potent anticancer derivatives

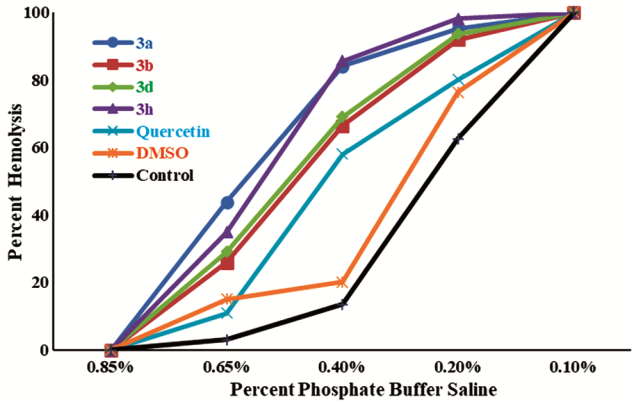

Fig. 3 — Erythrocyte osmotic fragility of isatin derivatives

differently with erythrocyte membranes, affecting their stability and haemolytic potential.

α-Glucosidase inhibition

The Rat intestinal α-glucosidase inhibitory activity was determined as per earlier reported methods[17]. As shown in Table 1, all the isatin analogues in which the triazole ring is attached to the benzyl group (3c-3i) exhibited either potent, significant or moderate inhibitory activity towards the enzyme AGH, but compounds in which the triazole ring is attached to the phenyl group (3a-3b) did not show activity. Amongst all, **3e** with 2,4 dichloro-benzyl-triazole ring has shown potent inhibitory activity (47.4%) followed by **3d** and **3h** with 3-chloro (35.6%) and 2-cyano (31.3%) substituted benzyl ring. Thus, it can be inferred that the presence of benzyl-triazole linkage is essential than the phenyl-triazole ring, and the presence of a chloro-substituted benzyl-triazole ring may be more ideal to generate α-glucosidase enzyme inhibitory activity.

Lipase inhibition

Lipase activity of the synthesized Isatin-triazole derivatives was evaluated *in vitro* mode as per the previous reports[18]. The findings demonstrated that, with the exception of three compounds (**3a, 3e,** and **3i**), the other compounds all shown strong, noteworthy, or moderate lipase inhibition action. Compounds **3f** with *para* fluoro-bezyl triazole ring, **3h** with *ortho* cyano-benzyltriazole have shown potent (80.8%) and significant (61.8%) activity compared to the standard Orlistat (91.1%) (Fig. 4). It can be seen that 4-fluoro benzyl substitution (**3f**) was more potent than 2-fluoro substitution (3g, 30.7%), similarly, 2-cyano benzyl (3h) was more potent than 2-cyano biphenyl substituted triazole (**3i**).

In silico Molecular Docking Studies

The docking result of **3d** with Histone deacetylase catalytic core (Fig. 5 and Table 2) showed that the inhibitor Vorinostat bound at the inhibitor Vorinostat binding pocket with a higher binding affinity of -8.0 kcalmol-1 than Vorinostat -7.7 kcalmol-1. Vorinostat interacts with the target by making only one H-bond through the amino acid residue TYR-297, whereas **3d** makes five H-bonds with amino acids GLY-295, TYR-297, GLY-129, GLN-254 and ASP-168, respectively. In case of cell line HepG2 the molecular interaction study of active derivatives **3a**, **3d** and **3h** on target topoisomerase IIα revealed that they bind well at control drug doxorubicin (-9.3 kcalmol-1) binding pocket (Fig. 6 and Table 3), **3d** exhibited highest binding affinity of -7.4 kcalmol-1 towards target compared to **3a** -6.8 kcalmol-1 and **3h** -6.6 kcalmol-1. For HeLa cell line compounds **3a**, **3b**, **3c** and **3h** were studied against target tubulin considering colchicine (-8.5 kcalmol-1) as control for binding energy assessment, the interaction study revealed that **3a**, **3b**, **3c** and **3h** docked well on the inhibitor binding site with binding affinity -7.8 kcalmol-1, -7.6 kcalmol-1, -7.5 kcalmol-1, and -7.3 kcalmol-1 respectively (Fig. 7 and Table 4). VAL-238 played an

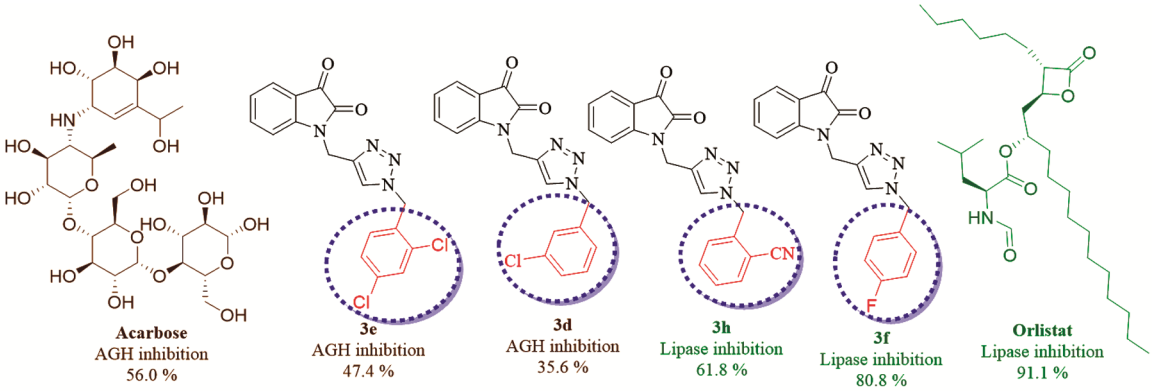

Fig. 4 — Structures of potent active derivatives against α-Glucosidase and lipase inhibition

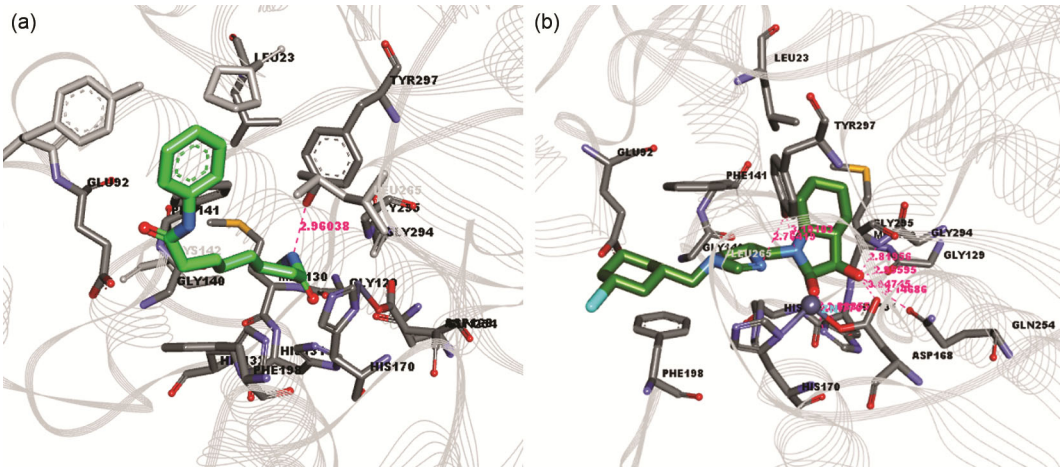

Fig. 5 — Binding pose of control inhibitor vorinostat and **3d** within the binding sit of histone deacetylase (a) docking pose of control Vorinostat at its inhibitor binding site by forming one hydrogen bond and (b) Docking pose of **3d** at vorinostat binding site forming five hydrogen bonds. Binding pocket residues are showed with gray stick form, Vorinostat, **3d** and hydrogen bonds are represented with green and pink colors respectively

Table 2 — Molecular docking interaction of vorinostat and **3d** with histone deacetylase catalytic binding site in terms of docking energy in kcalmol^{-1}.

Compd	A549, HDAC (PDB: 1C3S)	Docking binding energy kcal/mol	Binding site residues	Key residues (Å)
Vorinostat		–7.7	PRO-22, TYR-91, GLU-92, HIS-131, HIS-132, GLY-140, PHE-141, CYS-142, ASP-168, HIS-170, PHE-198, LEU-265, TYR-297	Tyr-297 (2.96038)
3d	7.72±0.07	–8.0	LEU-23, GLU-92, GLY-129, MET-130, HIS-131, HIS-132, GLY-140, PHE-141, CYS-142, ASP-168, HIS-170, PHE-198, GLN-254, LEU-265, GLY-294, GLY-295, TYR-297	GLY-295 (2.81956), TYR-297 (3.19102), GLY-129 (2.95595), GLN-254 (3.4686), ASP-168 (2.88855)

important role in ligand-target interaction. In case of ovarian carcinoma SKOV3 cell line active compound **3c** showed promising binding affinity of -10.2 kcalmol-1 against target PARP1 by forming three hydrogen bonds with amino acid ARG-878, SER-904, TRP-861, compared with control quinazoline-2,4(1*H*,3*H*)-dione (-13.1 kcalmol-1) by forming four hydrogen bonds (Fig. 8 and Table 5).

The Isatin derivative's ability to cross the blood-brain barrier (BBB) and Intestinal absorption was predicted by drawing a plot of Polar Surface Area (PSA) *versus* ALogP in 95% and 99% confidence limit ellipses (Fig. 9). PSA is a measure of the surface area of a molecule that is polar (*i.e.*, can form hydrogen bonds), while ALogP is a measure of the lipophilicity (or hydrophobicity) of a molecule.

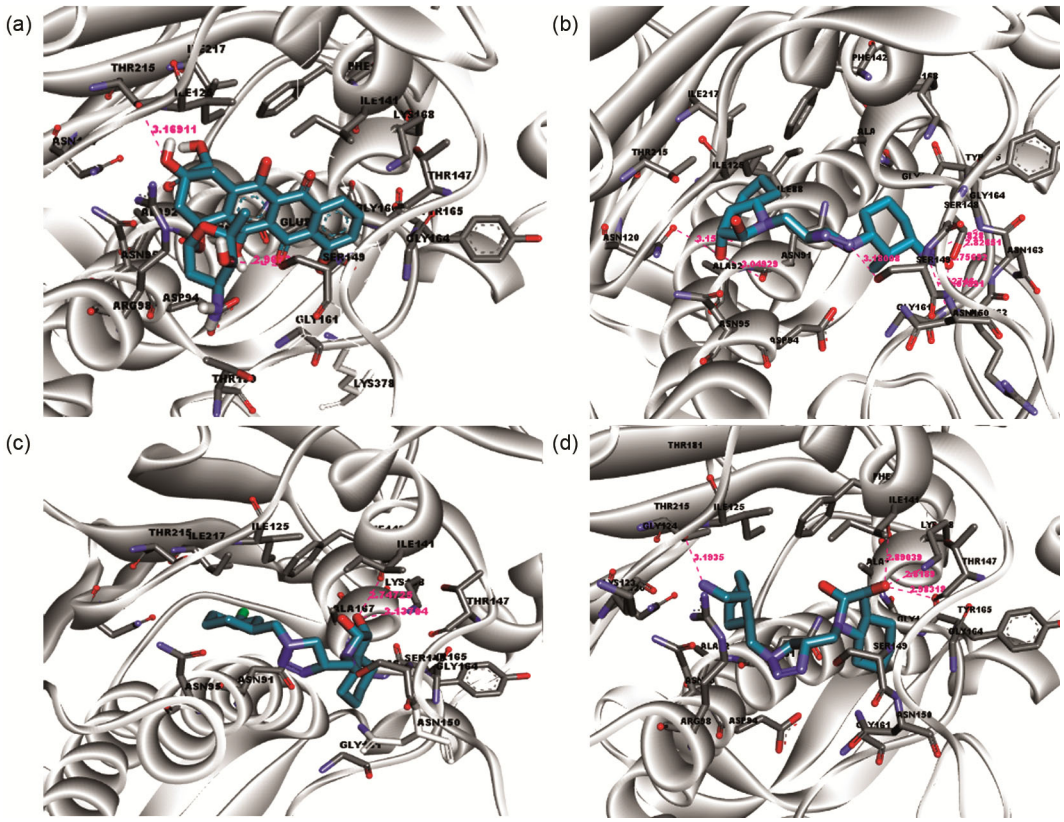

Fig. 6 — Binding pose of control inhibitor Doxorubicin, **3a**, **3d** and **3h** within the topoisomerase IIα binding site **(a)** docking pose of control Doxorubicin at its inhibitor binding site by forming two hydrogen bonds and **(b)** Docking pose of **3a** at the topoisomerase IIα binding site, forming six hydrogen bonds. **(c)** Docking pose of **3d** at topoisomerase IIα binding site forming two hydrogen bonds **(d)** Docking pose of **3h** at topoisomerase IIα binding site forming three hydrogen bonds. Binding pocket residues are shown with grey stick form, Doxorubicin, isatin derivatives and hydrogen bonds are represented with blue and pink colours, respectively

Table 3 — Molecular docking interaction of Doxorubicin, **3a**, **3d** and **3h** with topoisomerase IIα binding site in terms of docking energy in kcalmol^{-1}

Compd	HepG2,Topoisomerase IIα (PDB 1ZXM)	Docking binding energy kcal/mol	Binding site residues	Key residues (Å)
Doxorubicin	10.15±0.003	–9.3	GLU-87, ASN-91, ALA-92, ASP-94, ASN-95, ARG-95, ARG-98, ASN-120, ILE-125, ILE-141, PHE-142, THR-147, SER-149, THR-159, GLY-161, GLY-164, TYR-165, GLY-166, LYS-168, THR-215, ILE-217	SER-149 (2.96378), THR-215 (3.16911
3a	26.27±0.05	–6.8	ILE-88, ASN-91, ALA-92, ASP-94, ASN-95, ASN-120, ILE-125, PHE-142, SER-148, SER-149, ASN-150, GLY-161, ARG-162, ASN-163, GLY-164, TYR-165, THR-215, ILE-217,	SER-148, ARG-162, GLY-164, ASN-91, ASN-120, SER-148
3d	7.09±0.037	–7.4	ASN-91, ASN-95, ASN-120, ILE-125, ILE-141, PHE-142, THR-147, SER-149, ASN-150, GLY-161, GLY-164, TYR-165, GLY-166, ALA-167, LYS-168, THR-215, ILE-217	LYS-168 (3.13704), ILE-141 (2.74725)
3h	2.25±0.04	–6.6	ASN-91, ALA-92, ASP-94, ASN-95, ARG-98, ASN-120, LYS-123, ILE-125, , ILE-141, PHE-142, THR-147, SER-149, ASN-150, THR-147, SER-149, ASN-150, GLY-161, GLY-164, TYR-165, GLY-166, ALA-167, LYS-168, THR-215	LYS-168 (2.8189), THR-168 (3.1935), ILE-141 (2.89039)

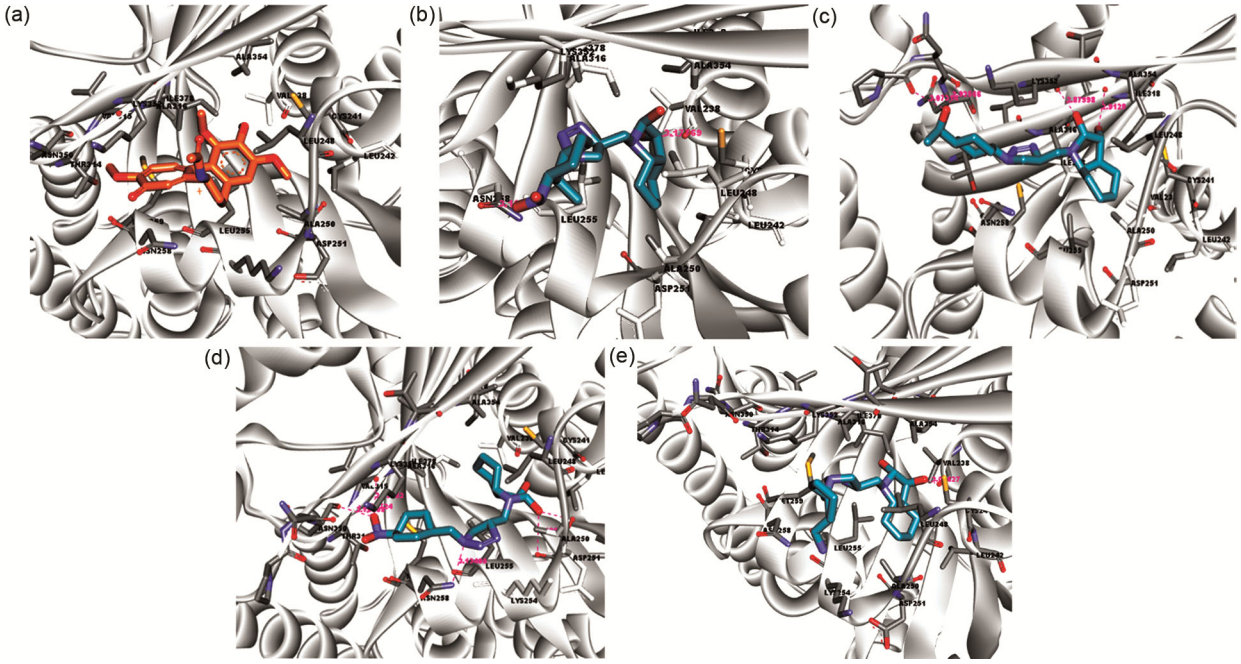

Fig. 7 — Binding pose of control inhibitor Colchicine, **3a-3c** and **3h** with tubulin binding site **(a)** docking pose of control compound Colchicine at its tubulin binding site **(b)** Docking pose of **3a** at its tubulin binding site forming two hydrogen bonds. **(c)** Docking pose of **3b** at the tubulin binding site, forming four hydrogen bonds (d), Docking pose of 3c at the tubulin binding site, forming four hydrogen bonds, and (e) Docking pose of 3h at the tubulin binding site, forming one hydrogen bond. Binding pocket residues are showed with gray stick form, colchicine, isatin derivatives and hydrogen bonds are represented with orange, blue and pink colors, respectively

Table 4 — Molecular docking interaction of Colchicine, **3a-3c** and **3h** with tubulin binding site in terms of docking energy in kcalmol^{-1}

Compd	HeLa, Tubulin (PDB 4O2B)	Docking binding energy kcal/mol	Binding site residues	Key residues (Å)
Colchicine		–8.5	CYS-241, LEU-248, ALA-250, ASP-251, LYS-– 254, LEU-255, ASN-258, MET-259, THR-314, VAL-315, ALA-316, ILE-318, ASN-350, LYS-352, ILE-378	
3a	6.52±0.04	–7.3	VAL-238, CYS-241, LEU-242, LEU-248, ALA-250, ASP-251, LEU-255, ASN-258, ALA-316, ILE-318, LYS-352, ALA-354, ILE-378	VAL-238 (3.17769), ASN-25 (3.1006)
3b	2.78±0.04	–7.8	CYS-241, LEU-248, LEU-255, ASN-258, MET-259, THR-314, VAL-315, ALA-316, ALA-317, ILE-318, PRO-348, ASN-349, ASN-350, LYS-352, THR-353, ALA-354	ALA-317 (2.9129), LYS-352 (2.7998), RO-348 (3.07314), ASN-349 (2.92566)
3c	28.85±0.29	–7.6	VAL-238, CYS-241, LEU-248, ALA-250, ASP-251, LYS-254, LEU-255, ASN-258, MET-259, THR-314, VAL-315, ALA-316, ILE-318, ASN-350, LYS-352, ILE-378,	ALA-250 (2.89689), ASP-251 (3.13824), VAL-315 (2.73182), ASN-350 (3.70208)
3h	88.16±0.01	–7.5	VAL-238, CYS-241, LEU-242, LEU-248, ALA-250, ASP-251, LYS-254, LEU-255, ASN-258, ALA-316, ILE-318, LYS-352, ILE-378,	VAL-238 (3.00628)

From the Fig. 9, Orlistat and Doxorubicin (control drugs) are used to compare the predicted results. Both controls are lying outside of 95 and 99% prediction models of humans (logP (oral bioavailability), Absorption, & BB Barrier - 95 & 99% confidence level- DS-TOPKAT v3.0, Accelrys/Biovia, USA). This shows that isatin derivatives are much better in terms of bioavailability as compare to controls, so that the failure chances are negligible (2-5%) in clinical trials.

Table 5 — Molecular docking interaction of quinazoline-2,4(1*H*,3*H*)-dione and **3c** with the PARP1 binding site in terms of docking energy in kcalmol^{-1}

Compd	SKOV3, PARP (PDB: 5WTC)	Docking binding energy kcal/mol	Binding site residues	Key residues (Å)
Quinazoline-2,4(1*H*,3*H*)-dione		–13.1	ASP-766, LEU-769, ASP-770, TRP-861, HIS-862, GLY-863, ARG-878, TYR-889, GLY-894, ILE-895, TYR-896, PHE-897, SER-904, TYR-907, GLU-988	GLY-63 (3.09391), TYR-896 (3.07716), SER-904 (3.06046), GLY-863 (2.88226)
3c	49.65±0.02	–10.2	ASP-766, ASP-770, TRP-861, HIS-862, GLY-863, LEU-877, ARG-878, ALA-880, TYR-896, PHE-897, ALA-898, LYS-903, SER-904, TYR-907	ARG-878 (3.19028), SER-904 (2.79016), TRP-861 (2.81011)

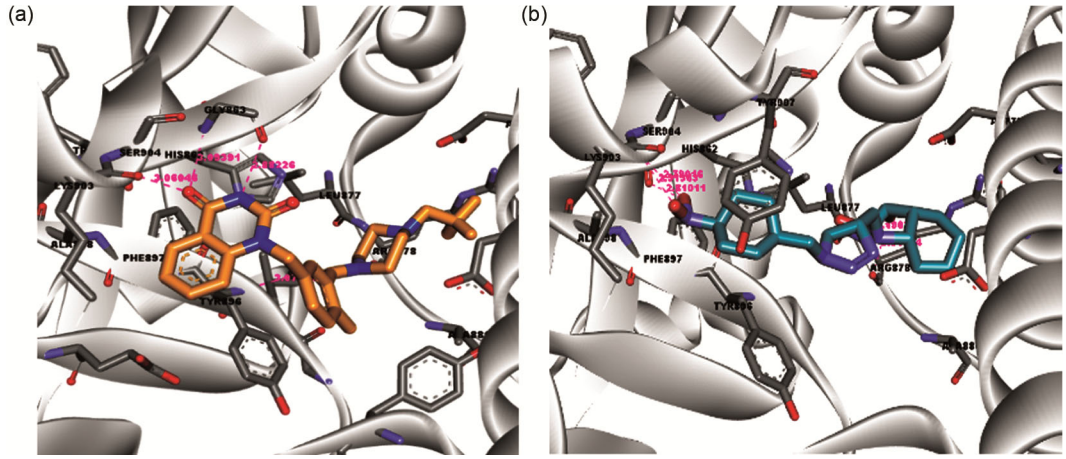

Fig. 8 — Binding pose of control inhibitor quinazoline-2,4(1*H*,3*H*)-dione and **3c** with PARP1 binding site **(a)** docking pose of control inhibitor quinazoline-2,4(1*H*,3*H*)-dione at its PARP1 binding site forming four hydrogen bonds **(b)** Docking pose of **3c** at its PARP1 binding site forming three hydrogen bonds. Binding pocket residues are shown with gray stick form, quinazoline-2,4(1*H*,3*H*)-dione, isatin derivative **3c** and hydrogen bonds are represented with orange, blue and pink colors, respectively

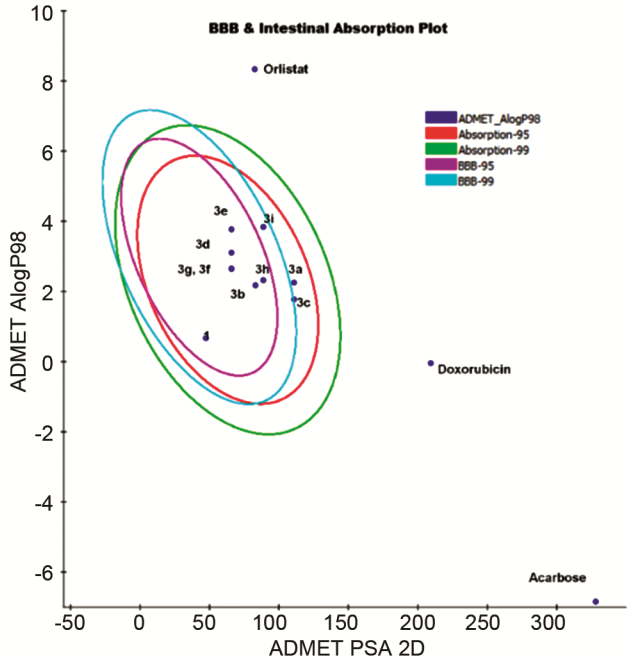

Fig. 9 — Plot of polar surface area (PSA) *versus* ALogP for Isatin triazole derivatives

The evaluation of inhibitory effects towards diabetic target alpha-glucosidase and the Evaluation of inhibitory effects towards lipase activity of docking studies are mentioned in Supplemental data.

Experimental Section

Chemistry

The synthetic strategy of isatin N-substituted 1,2,3-triazoles was outlined in our earlier studies[15].

In vitro anti cancer activity

Chemicals

Dulbecco's modified eagle medium (DMEM), , MTT [3-(4, 5- dimethylthiazol-2-yl)-2, 5-diphenyl tetrazolium bromide], trypsin-EDTA, Antibiotic antimycotic solution, Phosphate buffered saline (Ca2+, Mg2+ free; PBS), Dimethyl sulfoxide (DMSO) were purchased from Sigma Chemicals Co (St.Louis, MO, USA), Fetal bovine serum (FBS) were purchased from Gibco, USA, Cell culture 96 well plates and plastic wares were

obtained from Techno Plastic Products (TPP) (CH-8219 Trasadingen, Switzerland). All other chemicals were obtained locally and were of analytical grade.

Methods

Cell culture

Human lung adenocarcinoma cell line (A549), human hepatocarcinoma cell line (HepG2), Human breast carcinoma cell line (MCF-7), Human cervical cancer cell line (HeLa) and Human Ovarian carcinoma cell lines were obtained from American Type Culture Collection (ATCC) (Manassas, VA, USA). The cell lines were grown in DMEM medium supplemented with 10% FBS, 0.3% sodium bicarbonate, 10 mL/L antibiotic antimycotic solution (10,000 U/mL penicillin, 10 mg/mL streptomycin and 25µg/mL amphotericin B). The culture was maintained in a CO_2 incubator at 37°C with a 90% humidified atmosphere and 5% CO_2.

Preparation of samples for MTT assay

Test compounds were taken in 10 mg/mL of DMSO, and various dilutions were made with sterile PBS (1X) to get desired concentrations. All formulations were filtered with a 0.22 µm sterile filter and 20 minutes of UV eradication before adding to the 96-well plates containing cells.

Anticancer activity of the Isatin-N-1,2,3-triazole derivatives **3a-i** was evaluated *in vitro* using 3-(4,5-dimethylthiazol-2-yl)-2,5-diphenyltetrazolium bromide (MTT) assay[19] on the human cancer cell lines A549, HepG2, MCF-7, HeLa and SKOV3. The assay is based on the reduction of MTT by the mitochondrial dehydrogenase of viable cells into purple formazan crystals, which are dissolved in DMSO and read at 570 nm. Briefly, 1×10^4 exponentially growing cells were seeded into each 96 well plate (counted by Trypan blue exclusion dye method) allowed to grow till 60-70% confluence then compounds were added to the culture medium with the final concentrations ranging from 0.1, 1, 5 and 10 µM and along with controls (negative (without compound) and positive (Doxorubicin) incubated for 24 hours CO_2 incubator at 37°C with a 90% humidified atmosphere and 5% CO_2. Then the media of the wells were replaced with 90 µL of fresh serum-free media and 10 µL of MTT (5 mg/mL of PBS), plates were incubated at 37°C for 2 h, thereafter the above media was discarded and allowed to dry for 30 minutes. Add 100 µL of DMSO in each well at 37°C for 5 min. The purple formazan crystals were dissolved, and immediately, the absorbance at 570 nm was measured using a Spectra Max plus 384 UV-Visible plate reader (Molecular Devices, Sunnyvale, CA, USA). IC_{50} values were determined by % Cell viability (from control) *versus* concentration using the probit analysis software package of MS Excel.

α-Glucosidase inhibition

The Rat intestinal α-glucosidase inhibitory activity was determined as per earlier reported methods[20]. Rat intestinal acetone powder in normal saline (100:1; w/v) was sonicated properly, and the supernatant was used as a source of crude intestinal α-glucosidase after centrifugation. In brief, 10 mL of test samples (5 mg/mL DMSO solution) were reconstituted in 100 mL of 100 mM phosphate buffer (*p*H 6.8) in 96-well microplate and incubated with 50 mL yeast, α-glucosidase (0.76 U/Ml in same buffer) or crude intestinal α-glucosidase for 5 min before 50 mL substrate (5 mM, *p*-nitrophenyla-D-glucopyranoside prepared in same buffer) was added. Release of p-nitrophenol was measured at 405 nm spectrophotometrically ($Spectra_{MAx}$ Plus[384], Molecular Devices Corporation, Sunnyvale, CA, USA) 5 min after incubation with substrate. Individual blanks for test samples were prepared to correct background absorbance, where the substrate was replaced with 50 mL of buffer. The control sample contained 10 L of DMSO in place of the test samples. Acarbose was taken as a standard reference for α-glucosidase inhibition. All the samples were studied in triplicate. The percentage of enzyme inhibition was calculated as (1- B/A) x 100, where A represents the absorbance of the control without test samples, and B represents the absorbance in the presence of test samples. All the tests were run in duplicate.

Lipase inhibition

Lipase activity of the synthesised Isatin-triazole derivatives was evaluated in an *in vitro* mode as per the previous reports[21]; lipase from porcine pancreas Type II (Sigma product L3126) was dissolved in ultra-pure water at 10 mg/mL; then the supernatant was used after centrifugation at 16,000 rpm for 5 min. The assay buffer was 100 mM Tris buffer (*p*H 8.2), and *p*-nitrophenyl laurate (pNP laurate) was used as the substrate. The substrate stock 0.08% w/v pNP laurate was dissolved in 5 mM sodium acetate (*p*H 5.0) containing 1% Triton X-100 and was heated in boiling water for 1 min to aid dissolution, mixed

well, then cooled to RT. The control assay contained 400 µL assay buffer, 450 µL substrate solution and 150 µL lipase. The synthesised compounds were dissolved in DMSO (1 mg/mL) and added in a 50 µL total volume. The buffer, enzyme and compounds were added, and then the substrate was added to start the reaction. The samples were incubated at 37 °C for 2 h. Then, samples were centrifuged at 16,000 rpm for 2.5 min and read at 400 nm in a UV spectrophotometer. All samples were assayed in triplicate, and an inhibitor blank was prepared for each sample.

In silico Molecular Docking Studies

The binding affinity prediction and mechanistic exploration of isatin-based ten derivatives were performed against four cancer targets, *viz*., Histone deacetylases HDAC (A549), topoisomerase IIα (HepG2), tubulin (HeLa), and Poly (ADP-ribose) polymerases PARP (SKOV3). PDB codes for molecular docking studies are 1C3S, 1ZXM, 4O2B and 5WTC, respectively. The cancer target selection was done on the basis of bound inhibitor, crystal structure resolution, and published literatures.

Supplementary Information

Supplementary information is available in the website http://nopr.niscpr.res.in/handle/123456789/58776.

Acknowledgements

The authors thank the Director, CSIR-CIMAP, Lucknow, India, for his constant encouragement and support. CIMAP Publication Communication Number: CIMAP/PUB/2025/33.

References

1 Guo Y & Chen F, *Zhongcaoyao,* 17 (1986) 8.
2 Yoshikawa M, Murakami T, Kish A, Sakurama T, Mat-Suda H, Nomura M & Kubo M, *Chem Pharm Bull*, 46 (1998) 886.
3 Bergman J, Lindstrom J O & Tilstam U, *Tetrahedron,* 41 (1985) 2879.
4 Glover V, Reveley M A & Sandler M, *Biochem Pharm*, 29 (1980) 467.
5 Abo-Ashour M F, Eldehna W M, Nocentini A, Ibrahim H S, Bua S, Abou-Seri S M, Supuran C T, *Eur J Med Chem*, 157 (2018) 28.
6 Kamal A, Mahesh R, Nayak V L, Babu K S, Kumar G B, Shaik A B, Kapure J S & Alarifi A, *Eur J Med Chem*, 108 (2016) 476.
7 Eldehna W M, Kerdawy A M, Al-Ansary G H, Al-Rashood S T, Ali M M & Mahmoud A E, *Eur J Med Chem*, 163 (2019) 37.
8 Jeong P, Moon Y, Lee J H, Lee S D, Park J, Lee J, Kim J, Lee H J, Kim N Y, Choi J, Jeong D H, Eun S J, Hyun W P, Yoon-Gyoon K, Sun-Young H, Yong-Chul K, *Eur J Med Chem*, 195 (2020) 112205.
9 Ali A Q, Teoh S G, Eltayeb N E, Khadeer A M B, Abdul M A M S, *Polyhedron*, 74 (2014) 6.
10 Evdokimov N M, Magedov I V, McBrayer D, Kornienko A, *Bioorg Med Chem Lett*, 26 (2016) 1558.
11 Teng Y O, Zhao H Y, Wang J, Liu H, Le Gao M, Zhou Y, Han K L, Fan Z C, Zhang Y M, Sun H & Peng Y, *Eur J Med Chem*, 112 (2016) 145.
12 Meleddu R, Petrikaite V, Distinto S, Arridu A, Angius R, Serusi L, Škarnulytė L, Endriulaitytė U, Paškevičiūtė M, Cottiglia F. Marco G, Domenico T, Serenella D, Benedetta F & Elias M, *ACS Med Chem Lett*, 10 (2019) 571.
13 Xu Z, Song X, Hu Y, Qiang M & Lv Z, *J Heter Chem*, 55 (2018) 192.
14 Kumar K, Carrère-Kremer S, Kremer L, Guérardel Y, Biot C & Kumar V, *Organometallics*, 32 (2013) 5713.
15 Niranjana Kumar A, Smruti Ranjan D, Kotesh Kumar J, Srinivas K V N S & Sarada D T, *RSC Adv*. 15 (2025) 2023.
16 Mossman T, *J Immun Meth,* 65 (1983) 55.
17 Hansen M B, Nielsen S E & Berg K, *J Immun Meth,* 119 (1989) 203.
18 Gilham D & Lehner R *Methods*, 36 (2005) 139.
19 Dougall M G J, Shpiro F, Dobson P, Smith P & Blake A, *J Agri Food Chem*, 53 (2005) 2760.